RSC Advances

PAPER

View Article Online
View Journal | View Issue

Cite this: *RSC Adv.*, 2021, **11**, 14415

Bio-mineralisation, characterization, and stability of calcium carbonate containing organic matter†

Renlu Liu,[ab] Shanshan Huang,[b] Xiaowen Zhang,[b] Yongsheng Song,[a] Genhe He,*[a] Zaifeng Wang[b] and Bin Lian *[b]

The composition of organic matter in biogenic calcium carbonate has long been a mystery, and its role has not received sufficient attention. This study is aimed at elucidating the bio-mineralisation and stability of amorphous calcium carbonate (ACC) and vaterite containing organic matter, as induced by *Bacillus subtilis*. The results showed that the bacteria could induce various structural forms of $CaCO_3$, such as biogenic ACC (BACC) or biogenic vaterite (BV), using the bacterial cells as their template, and the carbonic anhydrase secreted by the bacteria plays an important role in the mineralisation of $CaCO_3$. The effects of Ca^{2+} concentration on the crystal structure of $CaCO_3$ were ascertained; when the amount of $CaCl_2$ increased from 0.1% (m/v) to 0.8% (m/v), the ACC was transformed to polycrystalline vaterite. The XRD results demonstrated that the ACC and vaterite have good stability in air or deionised water for one year, or even when heated to 200 °C or 300 °C for 2 h. Moreover, the FTIR results indicated that the BACC or BV is rich in organic matter, and the contents of organic matter in biogenic ACC and vaterite are 39.67 wt% and 28.47 wt%, respectively. The results of bio-mimetic mineralisation experiments suggest that the protein secreted by bacterial metabolism may be inclined to inhibit the formation of calcite, while polysaccharide may be inclined to promote the formation of vaterite. Our findings advance our knowledge of the $CaCO_3$ family and are valuable for future research into organic-$CaCO_3$ complexes.

Received 23rd January 2021
Accepted 7th April 2021

DOI: 10.1039/d1ra00615k

rsc.li/rsc-advances

1 Introduction

$CaCO_3$ comes from a variety of sources, and the mineralisation of $CaCO_3$ induced by microbes is an important source that cannot be ignored. These biogenic $CaCO_3$ crystals are normally nanometric, of diverse crystal types, wrapped in rich organic matter, and complex elemental compositions, differing from non-biogenic carbonates.[1–6] Calcium carbonate deposition is a common phenomenon in seawater, fresh water, soil, and other environments. Calcium carbonate generates seven structural forms: calcite, monohydrocalcite, ikaite, aragonite, vaterite, hemihydrate calcium carbonate, and amorphous calcium carbonate (ACC), among which calcite is the most stable structural form at normal temperature and pressure.[7–12] The process and mechanism of calcite biomineralisation have been researched deeply, but the research on the process and mechanisms of ACC and vaterite biomineralisation continues to be lacking.

Carbonic anhydrase (CA) was first found in human erythrocytes and is widely present in plants, animals, and microbes. CA is capable of catalyzing the reversible hydration reaction, $CO_2 + H_2O \leftrightharpoons H^+ + HCO_3^-$, of atmospheric and self-generated CO_2.[13] CA is currently recognised as being involved in carbonate synthesis.[13–15] Although bio-induce mineralisation of $CaCO_3$ is related to urease secreted by bacteria, but it requires the addition of urea as its substrate.[16–19] A variety of microbes, such as eukaryotic algae,[20,21] fungi,[22,23] and bacteria[3,12,24] can induce $CaCO_3$ mineralisation, however, the morphology and crystal structure of $CaCO_3$ induced by different microbes are quite different. Even the morphology and crystal structure of $CaCO_3$ induced by the same microbe are also quite different under different culturing conditions. ACC is normally a precursor of crystalline calcium carbonates that plays a key role in biomineralisation and polymorph evolution.[25] Where, the regulatory mechanism affecting the specific type of $CaCO_3$ (especially metastable ACC and vaterite) is far from clear in the case of microbial participation and further research into the directional induction mechanism of biogenic $CaCO_3$ is needed. Recent research has established that $CaCO_3$ precipitation induced by microbe contains organic components,[26,27] while the role of organic matter in the formation and structural stability (especially thermal stability) of biogenic mineral is rarely reported. Biogenic $CaCO_3$ has broad application prospects in biotechnology, civil engineering, and palaeontology.[10] Because

[a]*School of Life Sciences, Key Laboratory of Agricultural Environmental Pollution Prevention and Control in Red Soil Hilly Region of Jiangxi Province, Jinggangshan University, Ji'an 343009, China. E-mail: hegenhe@jgsu.edu.cn*

[b]*School of Life Sciences, School of Marine Science and Engineering, Nanjing Normal University, Nanjing 210023, China. E-mail: bin2368@vip.163.com*

† Electronic supplementary information (ESI) available. See DOI: 10.1039/d1ra00615k

the formation and precipitation of $CaCO_3$ lead to the deposition of atmospheric CO_2, or reduces CO_2 emissions in water or soil, it plays a positive role in reducing atmospheric CO_2 concentrations and retarding the greenhouse effect.[28–30] In addition, biogenic $CaCO_3$ has good adsorption properties for heavy metals,[5] and compared with abiotic calcium carbonate, it shows greater potential.[31] Our purpose is to elucidate the nucleation patterns and crystallisation processes involved and determine the composition and structure of biogenic $CaCO_3$. In addition, we hope to identify factors controlling biogenic $CaCO_3$ morphology, and discover how crystallisation parameters influence particle morphology in bacterial systems containing different concentrations of Ca^{2+} ions. The research is believed to be beneficial to the comprehensive exploitation and utilisation of the different types of biogenic $CaCO_3$.

Bacillus subtilis, as a popular strain used in microbial fertilisers, has been developed rapidly and widely in agricultural production across China.[5,32,33] During the process of bacterial culture, a large amount of ACC and vaterite precipitation was observed, which showed obvious biological effects. Although there are already some research reports on bacteria-induced carbonate, further study is still needed outlining the ACC and vaterite mineralisation micro-process induced by agricultural fertiliser strain. Here, the bacterial induction of ACC and vaterite mineralisation and its structural characteristics were researched, which will increase the understanding of biogenic calcium carbonate polymorphisms.

2 Materials and methods

2.1 Strain

Experimental strain: *B. subtilis* (GenBank accession number: KT343639) is China's official certified microbial fertiliser strain.[5,32] The strain is adapted to growth in neutral and weakly alkaline conditions. The bacterial colony is opaque, milk-white and yellowish, with a rough, folded surface and irregular edges; the bacteria are seen in short rod form, measuring about (0.6 to 0.8) μm × (1.2 to 1.6) μm.

2.2 The bacterial culture and related indicators for $CaCO_3$ bio-mineralisation

The *B. subtilis* was inoculated with two loops into 200 mL LB liquid medium (tryptone 1% (m/v), yeast extract 0.5% (m/v), NaCl 1% (m/v), $6.5 \leq pH \leq 7.5$), shaking-cultured at 30 °C and 180 rpm for about 10 h to prepare bacterial seed liquid [$(7.75 \pm 1.19) \times 10^7$ cfu mL^{-1}]. We prepared 100 mL of the modified LB medium (containing $CaCl_2$ 0.2 g, the $CaCl_2$ was added to the medium after separate sterilization) in a 250 mL Erlenmeyer flask to establish two groups: the experimental group (Group E1) (to which 2 mL bacterial seed liquid was added), and the control group (Group C) (to which 2 mL inactivated bacterial seed liquid was added, the bacterial seed liquid was inactivated at 115 °C for 20 min). At the same time, we prepared 100 mL of the LB medium in 250 mL Erlenmeyer flasks to form the E2 group (to which 2 mL bacterial seed liquid was added) as the control group without $CaCl_2$. Each group contained three replicates. These groups were then cultivated in a constant temperature oscillation incubator at 30 °C and 180 rpm for 0–14 days. The OD_{600nm} value of the culture solution was measured daily, then centrifuged at 8000 rpm for 15 min at 4 °C. The supernatant was used for the determination of HCO_3^- concentration,[34] Ca^{2+} concentration (atomic absorption spectrophotometer, AAS, AA-6300C, Shimadzu), pH (pH meter, SevenEasy S20), and CA activity.[34,35] We weighed the dry mass of precipitate from groups E1 and E2 after shaking-culturing for 7 days.

2.3 The role of CA in biogenic $CaCO_3$ mineralisation

Acetazolamide (AZ) is widely used as a CA inhibitor.[36,37] To clarify the role of CA in $CaCO_3$ mineralisation, different concentrations (0, 1.0, and 1.5 mg mL^{-1}) of AZ experimental groups were established and cultured at 30 °C and 180 rpm for 7 days. The centrifugal supernatant Ca^{2+} concentration was measured by AAS. Ignoring the Ca^{2+} utilised by the strain, most of the Ca^{2+} would be converted to $CaCO_3$, and then the Ca^{2+} biomineralisation efficiency was calculated by use of eqn (1):[38]

$$\text{Biomineralisation efficiency of } Ca^{2+}\ (\%) = \frac{C_1 - C_2}{C_1} \times 100 \quad (1)$$

where C_1 and C_2 are the initial, and end (after shaking-culturing for 7 days) concentrations of Ca^{2+} (mg L^{-1}), respectively.

2.4 The effect of Ca^{2+} concentrations on biogenic $CaCO_3$ mineralisation and its stability analysis

To explore the effect of Ca^{2+} concentration on biogenic $CaCO_3$ mineralisation, we added different amounts of $CaCl_2$ (0, 0.1, 0.2, 0.4, and 0.8 g) to 100 mL LB liquid culture medium, each group was dosed with 2 mL bacterial seed liquid, each group was cultured at 180 rpm for 7 days at 30 °C. The culture medium was centrifuged at 8000 rpm for 15 min after measuring the OD_{600nm} values and the number of bacterial cells. The supernatant Ca^{2+} concentration was determined by AAS, and the Ca^{2+} biomineralisation efficiency was calculated by use of eqn (1). We collected the precipitate, then added 5% HCl to observe whether there were any bubbles visible, preliminarily to determine whether there was any $CaCO_3$ present, or not. The sample was dropped on a clean cover glass and then observed by field emission scanning electron microscopy and energy dispersive spectrometry (FESEM-EDS, Zeiss Supra55) to analyse its morphology and elemental composition. Then, we determined the mineral structure by X-ray diffraction (XRD-526, Olympus, USA, using Co as the cathode) and transmission electron microscope-selected area electron diffraction (TEM-SAED, JEOL JEM-2000FX II). At the same time, the change in mineral structure was detected after the minerals were preserved at room temperature or shaken in deionised water for one year. The extraction method of organic matter in the $CaCO_3$ refers to Lv *et al.*[39]. Analysis of organic matter was undertaken by Fourier transform infrared spectrophotometer (FTIR, Nexus670, Thermo Nicolet), and the content of organic matter in biogenic $CaCO_3$ was investigated by TGA (Perkin-Elmer, USA). The elemental and organic molecules of biogenic $CaCO_3$ were determined by X-ray photoelectron spectroscopy (XPS, ESCALAB Xi+).

To assess the stability of the structure of $CaCO_3$, the precipitates were heated for 2 hours in a high-temperature resistance furnace at 200 °C and 300 °C, and then the changes to the mineral phase structure before and after heating were detected by XRD.

2.5 Bio-mimetic mineralisation of $CaCO_3$

The bio-mimetic mineralisation experiments were conducted to explore the effect of organic matter on the formation of biogenic $CaCO_3$. Salt solution A consisted of 0.2 mol L^{-1} $NaHCO_3$ and 0.2 mol L^{-1} $CaCl_2$. The pH of solution A was adjusted to 3.0 using 0.5 mol L^{-1} HCl, and then it was filtered through a 0.22 μm filter. Solution B is a series of 5 mL solution with different organic components, which are bacterial extracellular protein, extracellular polysaccharide (EPS), fermentation supernatant, glucose, sucrose, or bovine serum albumin. The *B. subtilis* was cultured in LB liquid medium at 30 °C and 180 rpm for 3 days. The methods for extraction of bacterial crude extracellular protein and EPS were based on those of Sánchez *et al.*[40] and Du *et al.*,[41] respectively. The culture solution was centrifuged at 8000 rpm for

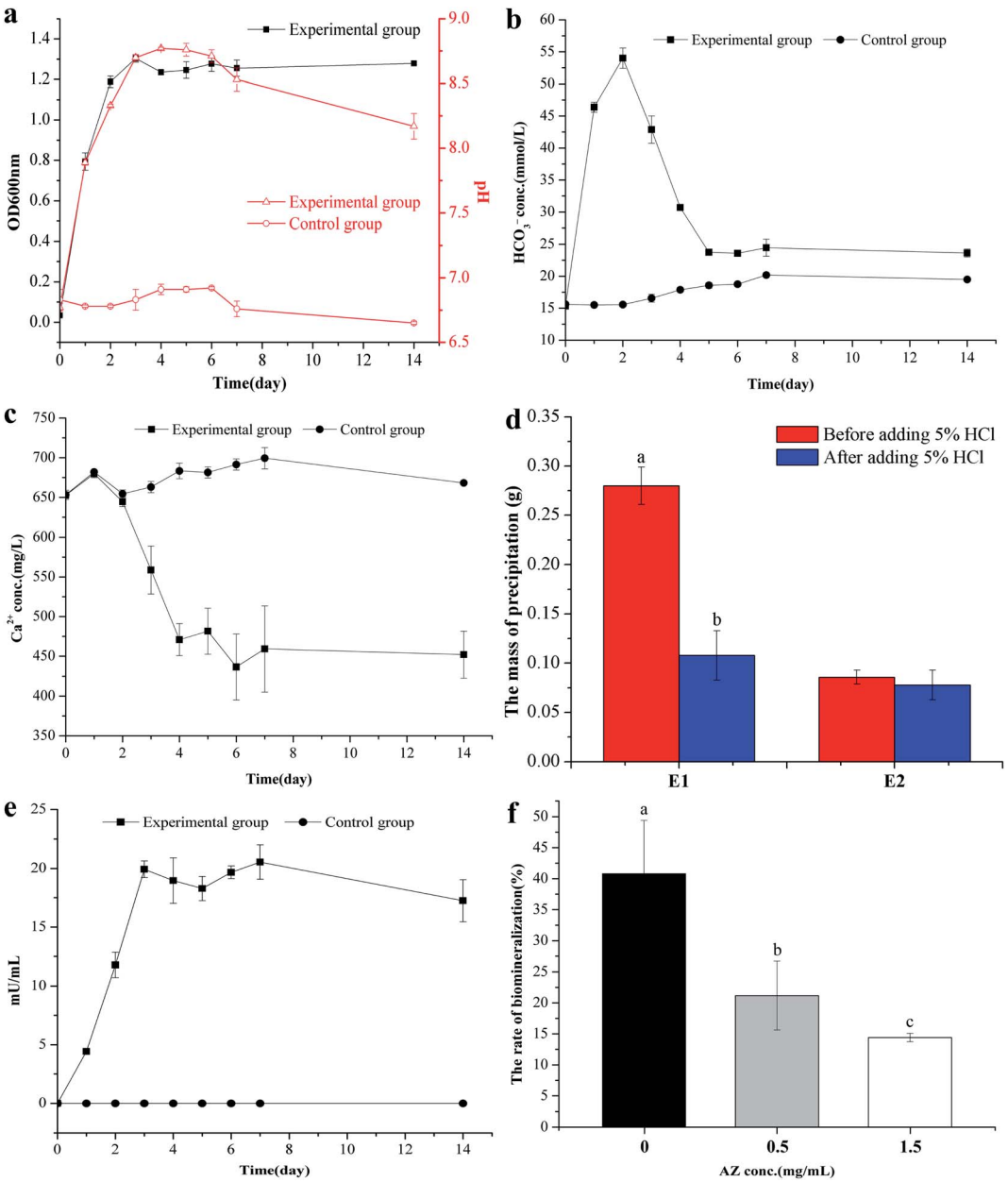

Fig. 1 The dynamic changes of physiological and chemical indexes in the process of calcium carbonate biomineralisation. (a) Change in OD_{600nm} and pH with time. (b) Change in HCO_3^- concentration with time. (c) Change in Ca^{2+} concentration with time. (d) The precipitated mass of E1 and E2 group (E1 group: with 0.2% (m/v) $CaCl_2$, E2 group: without $CaCl_2$) (bars with different letters indicate statistically significant differences, *t*-test, $p < 0.01$). (e) Change in CA activity with time. (f) The biomineralisation efficiency of Ca^{2+} after adding CA inhibitors (AZ) (bars with different letters represent statistically significant differences, one-way ANOVA, Duncan's multiple range test, $p < 0.05$). Data represent mean ± standard deviation (s.d.) of three independent experiments.

10 min and the supernatant was filtered through a 0.22 μm filter to remove cells. Solution B was added to 15 mL of solution A to form a series of mineralisation systems. The control group was set with 15 mL solution A and 5 mL distilled water. The mineralisation experimental device referred to that used in Lian *et al.*[3] All the experiments were run in triplicate. The precipitation products were collected by centrifugation (8000 rpm, 15 min) after 14 days and dried at 55 °C for XRD analysis.

3 Results and discussion

3.1 Bacterial culture and related indicators of $CaCO_3$ biomineralisation

B. subtilis grew rapidly in the LB medium, and on the third day, the OD_{600nm} value had reached 1.30 (Fig. 1a). The rapid growth of the bacterium lead to the change of the pH value in the bacterial culture: the maximum pH value was 8.77 on the third day in the experimental group (added 2 mL bacterial seed liquid), which increased by 2 compared with the initial value ($p < 0.01$). However, the pH value in the control group (added 2 mL inactivated bacterial seed liquid) remained at 6.8 (its original value, Fig. 1a). It can be concluded that the pH increase is due to the ammonia released by the bacterial growth to degrade the proteins in the mediu.[42] The HCO_3^- concentration of the experimental group first increased up to a maximum (5.4×10^{-4} mol L^{-1}) at the second day, and then fell to 2.38×10^{-4} mol L^{-1} at the fifth day, whereas the HCO_3^- concentration in the control group remained quasi-constant (Fig. 1b). The Ca^{2+} concentration in the experimental group remained almost unchanged in the first two days and continuously decreased in the following 3 days: the Ca^{2+} concentration decreased to about 240 mg L^{-1} ($p < 0.01$), while the concentration of Ca^{2+} in the control group was unchanged (Fig. 1c). The E1 group (added 2 mL bacterial seed liquid) had obvious precipitation, and bubbled after adding 5% HCl (Fig. S1a†), which suggested that the precipitation in the E1 group contained a lot of $CaCO_3$. While there was no precipitation in the CK group (added 2 mL inactivated bacterial seed liquid) as shown in Fig. S1b.† The dry mass of the precipitation was also significantly higher than that of the E2 group without $CaCl_2$ ($p < 0.01$), and we found that the dry mass of the precipitate significantly decreased after adding 5% HCl (Fig. 1d). To sum up, we can deduce that the bacteria can induce the formation of $CaCO_3$, and Ca^{2+} concentration decreased owing to the formation of $CaCO_3$ by precipitation.

By measuring the activity of CA, we found that the CA activity in the experimental group increased over time and reached a maximum on the third day, thereafter, it remained almost

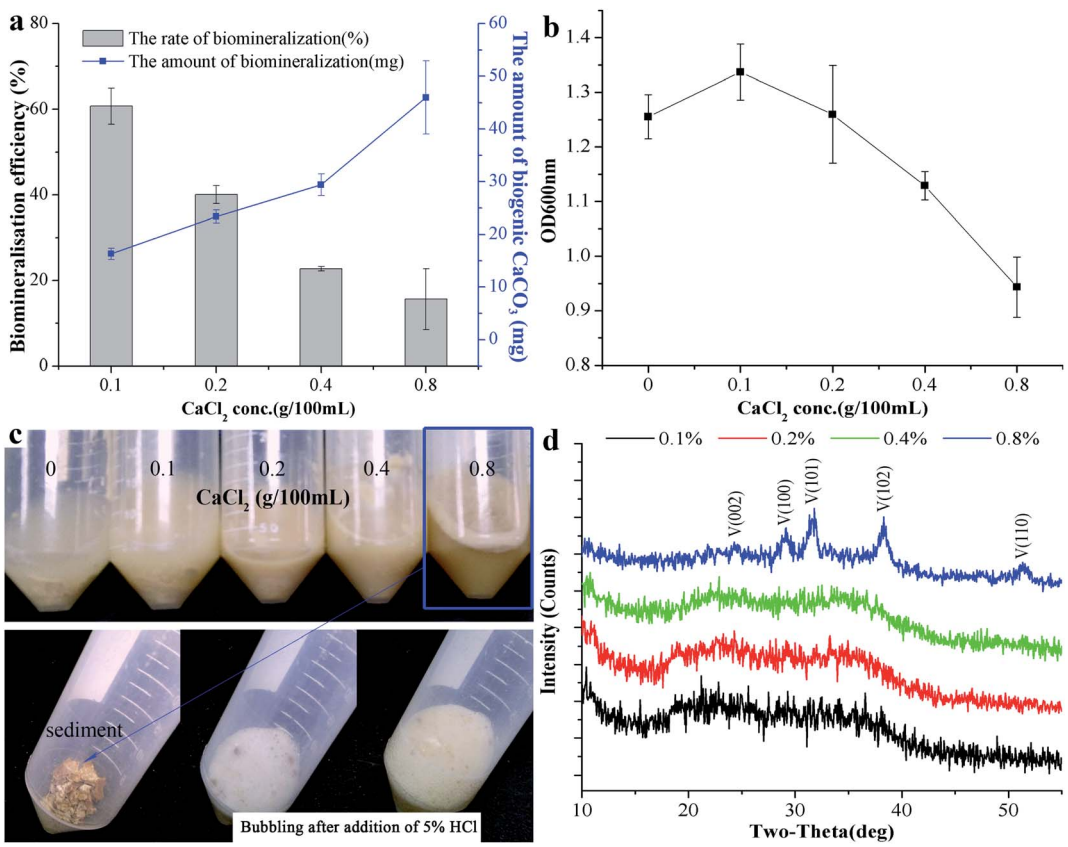

Fig. 2 The effect of different Ca^{2+} concentrations on $CaCO_3$ mineralisation. (a) The biomineralisation efficiency and amount of biogenic $CaCO_3$. (b) The OD_{600nm} of the bacterial culture at different amounts of added $CaCl_2$ after 7 days. (c) The precipitated reaction phenomenon after adding 5% HCl. (d) XRD results for the precipitate of different doses of $CaCl_2$. V: vaterite, ICDD pdf no. 72-0506. Data represent mean ± s.d. of three independent experiments.

constant (Fig. 1e), however, there was no microbial metabolism in the control group, so the activity of CA was not detected. For the role of CA on the formation of $CaCO_3$, Fig. 1f showed that the biomineralisation efficiency of Ca^{2+} decreased after adding CA inhibitor (AZ), and the biomineralisation efficiency of Ca^{2+} decreased with the increase of AZ concentration, which suggested that bacterial CA secretion is essential for the formation of $CaCO_3$.

3.2 The effect of Ca^{2+} concentration on $CaCO_3$ bio-mineralisation

The above research demonstrates that *B. subtilis* can induce biogenic $CaCO_3$ formation in an environment containing Ca^{2+}, but the concentration of Ca^{2+} in the environment is quite different, which may affect $CaCO_3$ bio-mineralisation. To clarify the mechanism of biogenic $CaCO_3$ mineralisation, experimental groups with different added amounts of $CaCl_2$ [0, 0.1, 0.2, 0.4, and 0.8% (m/v)] were established to identify the differences in $CaCO_3$ bio-mineralisation in bacterial systems containing different concentrations of Ca^{2+}. Fig. 2a showed that the Ca^{2+} mineralisation rate decreased with increasing Ca^{2+} increasing. However, the amount of mineralisation increased with the increase of Ca^{2+} concentration. The mineralisation reached a maximum (45.96 ± 6.95 mg) when the added amount of $CaCl_2$ was 0.8% (m/v). The OD_{600nm} gradually decreased with the increase in amount of $CaCl_2$, and the number of bacterial cell decreased from $(9.52 \pm 0.86) \times 10^7$ cfu mL^{-1} to $(6.22 \pm 0.93) \times 10^7$ cfu mL^{-1}, which was due to excessive Ca^{2+} inhibiting bacterial growth (Fig. 2b). 5% HCl was used to test the sediment in each group, and the results showed that the group without added $CaCl_2$ was free of bubbles, while groups with 0.1%, 0.2%, and 0.4% (m/v) $CaCl_2$ produced a few bubbles. Groups with 0.8% (m/v) $CaCl_2$ bubbled copiously, indicating the presence of different amounts of biogenic $CaCO_3$ at different doses of $CaCl_2$ (Fig. 2c). In addition, the XRD result shows that, with the increase of $CaCl_2$ dosing, the $CaCO_3$ induced by this strain can gradually be transformed from ACC to vaterite (ICDD pdf no. 72-0506) (Fig. 2d). To sum up, the morphism and structure of biogenic $CaCO_3$ will be affected by different Ca^{2+} concentration.

3.3 The morphology and mineralogical composition of biogenic $CaCO_3$

FESEM and TEM were utilized to observe the sediment after culturing for 7 days. We could observe some micro and nano-sized $CaCO_3$ with different morphologies, such as irregular, scaly aggregates, dumbbell-shaped, and spherical: their surfaces were mainly porous or corner-incomplete (Fig. 3a and b). From the enlarged FESEM image (Fig. 3b), the quasi-spherical $CaCO_3$ particles were rough-edged and were mainly formed by stacking nano-particles. The diameters of $CaCO_3$

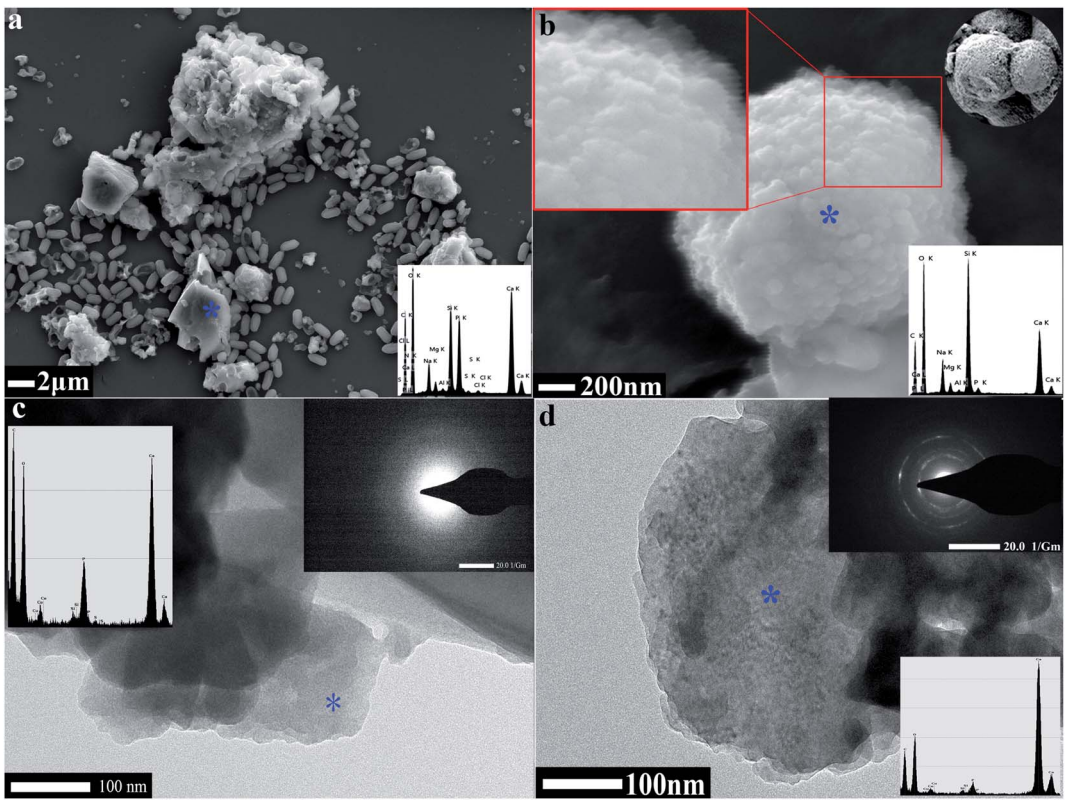

Fig. 3 Morphology and mineralogical analyses of $CaCO_3$. (a) FESEM-EDS result of $CaCO_3$ in 0.2% (m/v) $CaCl_2$ group. (b) FESEM-EDS result of $CaCO_3$ in 0.8% (m/v) $CaCl_2$ group. (c) TEM-SAED result of $CaCO_3$ in 0.2% (m/v) $CaCl_2$ group. (d) TEM-SAED result of $CaCO_3$ in 0.8% (m/v) $CaCl_2$ group.

particles or their aggregates were between 100 nm and 14 μm from 10 different recorded SEM and TEM visual images. The $CaCO_3$ in the culture system containing 0.2% (m/v) $CaCl_2$ revealed poorly resolved diffuse rings under TEM-SAED (Fig. 3c), and the XRD analysis shows no obvious diffraction peak (Fig. 2d), which demonstrates that the $CaCO_3$ was formed as ACC.[25,43,44] However, the $CaCO_3$ in the group containing 0.8% (m/v) $CaCl_2$ shows evident diffraction rings under TEM-SAED (Fig. 3d), which suggests that the $CaCO_3$ had formed a polycrystalline ring structure with a greater degree of crystallisation;[43] and the XRD result showed that the $CaCO_3$ was mainly composed of vaterite (Fig. 2d).

3.4 The stability analysis of biogenic ACC and vaterite structures

ACC serves as a precursor in the biomineralisation of almost all types of biogenic calcium carbonate.[45] Generally, ACC and vaterite will transform into a stable phase of calcite under certain conditions.[39,46,47] However, the XRD patterns of biogenic ACC or vaterite have no change in either air or deionised water over one year (Fig. 4a), or even heated to 200 °C or 300 °C for 2 h (Fig. 4b and c). Obviously, the biogenic ACC here is very different with the reported laboratory-produced ACC that needs to be stored in a desiccator below 10 °C for avoiding crystallization[48] or stable for half year at room temperature.[25] In addition, FTIR results (Fig. 4d) of the ACC and vaterite extracts suggest that there are some absorption peaks corresponding to diverse organic functional groups (including: –OH, $–CH_3$, $–CH_2$, –CO/NH, C=O, –COOH, and –NH).[39,49–51] Thus, we can infer that there are some organic compounds combined with the ACC and vaterite, forming an organic–inorganic complex structure. The TGA results show that, the calcium carbonate induced by the bacteria undergoes a mass-loss stage caused by organic matter combustion (within the range of 209–579 °C), compared to AR (Analytical Reagent)-$CaCO_3$ (purchased from Shanghai Sangon Biotech Co., Ltd) and limestone (provided by the Institute of Geochemistry, Chinese Academy of Sciences). And the contents of organic matter in biogenic ACC and vaterite are 39.67 wt% and 28.47 wt%, respectively (Fig. 5a and b), which are markedly higher than that in biogenic calcium carbonate (1.87 wt% and 6.82 wt%) induced by other strains.[26,27]

Moreover, the surface elementary compositions of the biogenic vaterite were determined by XPS over the energy range of 0–1200 eV. As showed in Fig. S2a,† the typical XPS survey spectrum shows that the core level peaks are C 1s (284.8 eV), O 1s (531.8 eV), Ca 2p (346.8 eV), and N 1s (399.8 eV). The mass

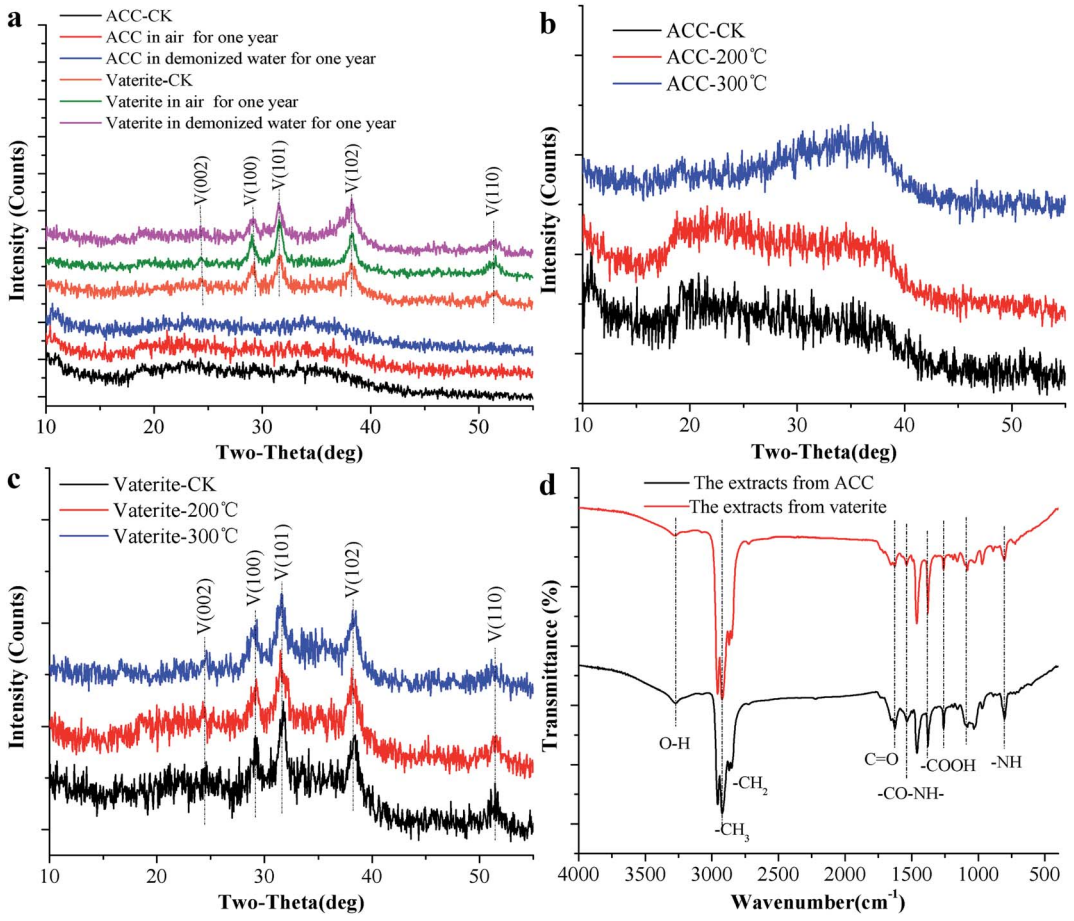

Fig. 4 The stability analysis of ACC and vaterite. (a) XRD patterns of ACC and vaterite under different conditions. (b) FTIR spectra of extracts from ACC and vaterite. (c) XRD patterns of ACC at different temperatures. (d) XRD patterns of vaterite at different temperatures.

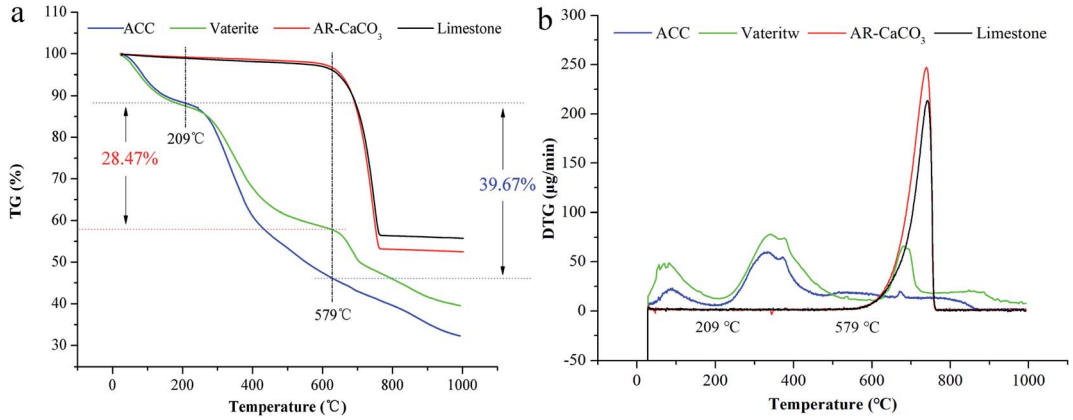

Fig. 5 TGA (a) and DTG (b) results: ACC, vaterite, AR-$CaCO_3$, and limestone.

fractions of C, O, Ca, and N were estimated about 62.76%, 27.59%, 5.12%, and 4.53%, respectively. Here, all three elements comprising $CaCO_3$, *i.e.* Ca, C, and O, as well as N which should come from organic matter were observed. The high-resolution XPS Ca 2p core-level spectrum has two peaks, identified as Ca $2p_{3/2}$ (347.1 eV) and Ca $2p_{1/2}$ (350.6 eV) (Fig. S2b†), and is in agreement with the reported value of vaterite.[52] To clarify the organic molecules involved in vaterite mineralisation, high resolution scans of C 1s and O 1s were deconvoluted, and the corresponding functional groups were recognized as C–(C/H), C–OH, C–O–C, C═O and O–C═O. Fig. S2c and d† depict the presence of three C (1s) and two O (1s). To clarify the organic molecules involved in vaterite mineralisation, high resolution scans of C 1s, and O 1s were deconvoluted, and the corresponding functional groups were recognized. The C 1s peak was resolved into three component peaks, *i.e.*, the peak at 284.6 eV (58.89%) can correspond to the C–(C/H) from lipids or amino acid side chains, the peak at 285.9 eV (24.76%) to C–OH or C–O–C from alcohol, ether, or phenol, the peak at 288.3 eV (16.35%) to $CaCO_3$, respectively. The O 1s peak at 531.5 eV (82.19%) can be assigned to $CaCO_3$, or C═O and O–C═O from carboxylic acid, carboxylate, carbonyl,

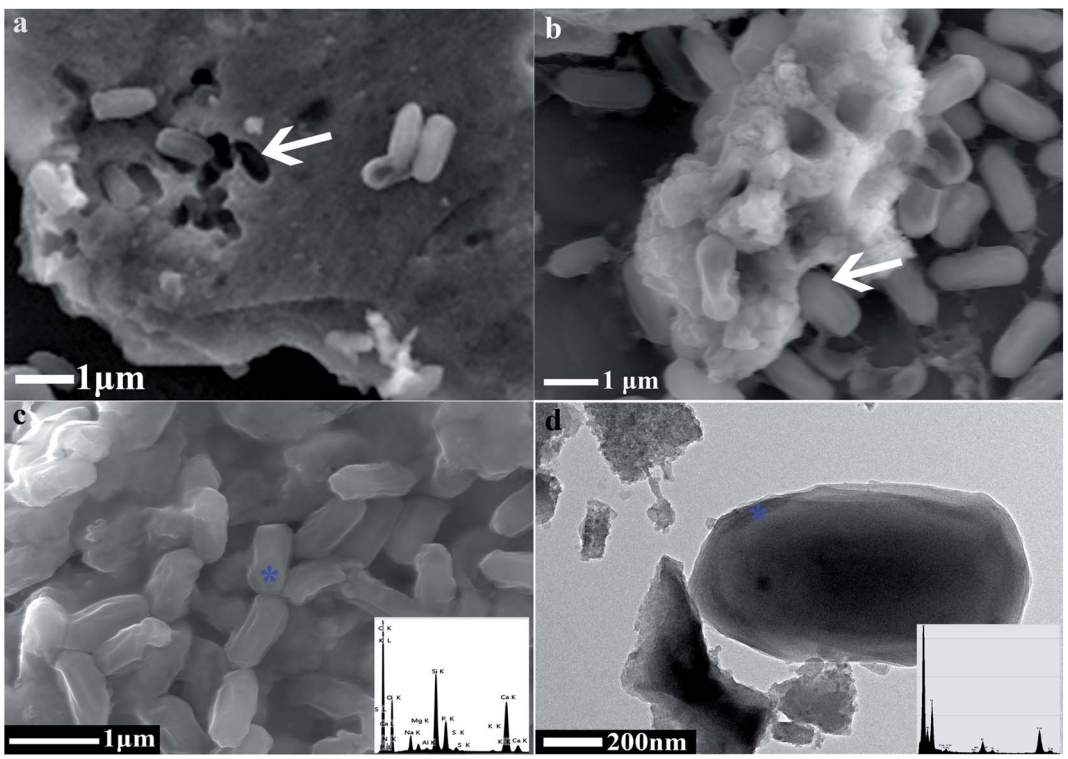

Fig. 6 The moulage caused by the bacteria on the $CaCO_3$ surface and calcified bacterial cells. (a and b) The FESEM images of moulage left by the bacteria and embedded bacterial cells on the surface of $CaCO_3$. (c) The FESEM-EDS of calcified bacterial cells. (d) The TEM-EDS of calcified bacterial cells.

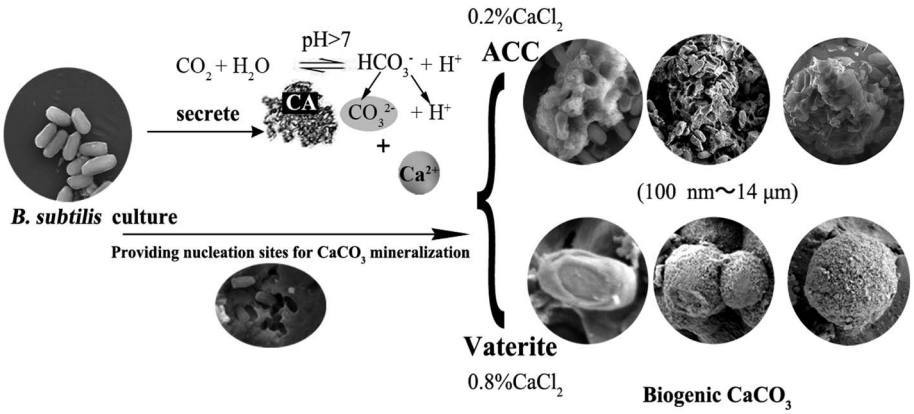

Fig. 7 The possible schematic mechanisms of $CaCO_3$ bio-mineralisation.

or amide.[26,53,54] The second O 1s peak at 533.2 eV (17.81%) is associated with C–OH or C–O–C from alcohol, acetal, and hemiacetal.[53,55] These organic matters are enwrapped by ACC and vaterite and can restrain their transformation into stable calcite.[2,3,26,39,56] The XRD patterns of products obtained by biomimetic mineralisation further confirm our speculation. From the XRD patterns (Fig. S3†), vaterite can be collected in most systems except those containing bovine serum albumin and distilled water. In other words, vaterite can only form in the presence of carbohydrate (crude extracellular protein contains some polysaccharide). Interestingly, the diffraction peaks of calcite harvested in systems with proteins were weaker than those in the control group. The results suggest that protein may be inclined to inhibit the formation of calcite, while polysaccharide may be inclined to promote the formation of vaterite. Hence, extracellular polysaccharide and protein secreted by bacterial metabolism maintain the stability of vaterite.

3.5 The micro-mechanism underpinning the formation of biogenic $CaCO_3$

The bio-mineralisation site of $CaCO_3$ synthesis has always a focus among researchers in this discipline.[3,39,57] We found that the bacteria were inserted in the $CaCO_3$ particles and left obvious moulages on their surface (Fig. 6a and b), which suggested that the extracellular structural substances of the bacteria play an important role in $CaCO_3$ formation or growth. Meanwhile, we observed many calcified bacterial cells with some irregular micro-grooves on the bacterial surfaces by FESEM, and the EDS results showed the presence of $CaCO_3$ on the bacterial surfaces (Fig. 6c). Moreover, the TEM image showed that the $CaCO_3$ not only forms in the regions surrounding the bacterial cells, but also forms directly on the surface of the bacterial cells (Fig. 6d). It is possible that Ca^{2+} was attracted by the negatively charged groups on the surface of bacteria especially at each of the two ends of the bacterium, then CO_3^{2-} was attracted through the cationic bridge[58–60] thus leading to the formation of various types of $CaCO_3$ (dumbbell type being the most common). CA was to catalyze the hydration of carbon dioxide, and this process released carbonate and bicarbonate ions that not only increased pH but also elevated carbonate supersaturation.[42] Therefore, we can infer that the bacterial exterior may be a good natural mineralising site, and the alkaline environment formed by bacteria can enhance the mineralisation on the bacterial surface. A spherical form of $CaCO_3$ can be grown by the transformation of dumbbell type $CaCO_3$ using a bacterial cell as the nucleation site.[61,62] In summary, the mechanism and process of $CaCO_3$ mineralisation are illustrated in Fig. 7.

4 Conclusions

This research found that *B. subtilis* could induce ACC or polycrystalline vaterite formation according to different Ca^{2+} concentration, which has long-term water stability and thermal stability. The stability of ACC and vaterite is closely related to the protein and extracellular polysaccharide secreted by the bacterium. The protein may be inclined to inhibit the formation of calcite, and the polysaccharide may be inclined to promote the formation of vaterite. The final morphology and structure of carbonate depends on the interaction between the protein and extracellular polysaccharide. Meanwhile, the bacterial cells, alkaline metabolites, and CA are important to the $CaCO_3$ bio-mineralisation process. The discovery of ACC and vaterite, their formation pathways, and the determination of their organic–inorganic structures broadens our knowledge of the mechanism of bio-mineralisation and provides reference for the exploitation and application of biogenic $CaCO_3$.

Conflicts of interest

There are no con conflicts to declare.

Acknowledgements

This work was supported by the National Key Technology R&D Program of China (Grant no. 2019YFC180510303), the Jiangsu Provincial Marine Science and Technology Innovation Special Project (Grant no. HY2019-3), the National Natural Science Foundation of China (Grant no. 41867032) and the Jiangxi

Provincial Natural Science Foundation (Grant no. 20202BABL215028).

References

1 C. Cao, J. Jiang, H. Sun, Y. Huang, F. Tao and B. Lian, Carbonate mineral formation under the influence of limestone-colonizing *Actinobacteria*: morphology and polymorphism, *Front. Microbiol.*, 2016, **7**, 366.

2 M. Kawano and J. Hwang, Roles of microbial acidic polysaccharides in precipitation rate and polymorph of calcium carbonate minerals, *Appl. Clay Sci.*, 2011, **51**, 484–490.

3 B. Lian, Q. Hu, J. Chen, J. Ji and H. H. Teng, Carbonate biomineralization induced by soil bacterium *Bacillus megaterium*, *Geochim. Cosmochim. Acta*, 2006, **70**, 5522–5535.

4 M. Obst, B. Wehrli and M. Dittrich, $CaCO_3$ nucleation by cyanobacteria: laboratory evidence for a passive, surface-induced mechanism, *Geobiology*, 2009, **7**, 324–347.

5 R. Liu, Y. Guan, L. Chen and B. Lian, Adsorption and desorption characteristics of Cd^{2+} and Pb^{2+} by micro and nano-sized biogenic $CaCO_3$, *Front. Microbiol.*, 2018, **9**, 41.

6 F. Héctor, G. Mónica, A. Bonifacio, I. Aldo and A. Marisela, Novel method to achieve crystallinity of calcite by *Bacillus subtilis* in coupled and non-coupled calcium-carbon sources, *AMB Express*, 2020, **10**, 1–20.

7 F. Giuseppe, F. Simona, R. Michela, N. D. A. Branka and K. Damir, Evidence of structural variability among synthetic and biogenic vaterite, *Chem. Commun.*, 2014, **50**, 15370–15373.

8 G. Zhou, Y. Guan, Q. Yao and S. Fu, Biomimetic mineralization of prismatic calcite mesocrystals: Relevance to biomineralization, *Chem. Geol.*, 2010, **279**, 63–72.

9 E. Bauerlein, Biomineralization of unicellular organisms: An unusual membrane biochemistry for the production of inorganic nano- and microstructures, *Angew. Chem., Int. Ed.*, 2003, **42**, 614–641.

10 N. K. Dhami, M. S. Reddy and A. Mukherjee, Biomineralization of calcium carbonates and their engineered applications: a review, *Front. Microbiol.*, 2013, **4**, 314.

11 Z. Zou, W. J. E. M. Habraken, G. Matveeva, A. C. S. Jensen, L. Bertinetti, M. A. Hood, C. Sun, P. U. P. A. Gilbert, I. Polishchuk, B. Pokroy, J. Mahamid, Y. Politi, S. Weiner, P. Werner, S. Bette, R. Dinnebier, U. Kolb, E. Zolotoyabko and P. Fratzl, A hydrated crystalline calcium carbonate phase: Calcium carbonate hemihydrate, *Science*, 2019, **363**, 396–400.

12 R. Rautela and S. Rawat, Analysis and optimization of process parameters for *in vitro* biomineralization of $CaCO_3$ by *Klebsiella pneumoniae*, isolated from a stalactite from the sahastradhara cave, *RSC Adv.*, 2020, **10**, 8470–8479.

13 B. C. Tripp, K. Smith and J. G. Ferry, Carbonic anhydrase: new insights for an ancient enzyme, *J. Biol. Chem.*, 2001, **276**, 48615–48618.

14 I. M. Power, A. L. Harrison and G. M. Dipple, Accelerating mineral carbonation using carbonic anhydrase, *Environ. Sci. Technol.*, 2016, **50**, 2610–2618.

15 Q. Sun and B. Lian, The different roles of *Aspergillus nidulans* carbonic anhydrases in wollastonite weathering accompanied by carbonation, *Geochim. Cosmochim. Acta*, 2019, **244**, 437–450.

16 S. Stocks-Fischer, J. K. Galinat and S. S. Bang, Microbiological precipitation of $CaCO_3$, *Soil Biol. Biochem.*, 1999, **31**, 1563–1571.

17 F. Hammes, N. Boon, J. de Villiers, W. Verstraete and S. D. Siciliano, Strain-specific ureolytic microbial calcium carbonate precipitation, *Appl. Environ. Microbiol.*, 2003, **69**, 4901–4909.

18 T. O. Okyay, H. N. Nguyen, S. L. Castro and D. F. Rodrigues, CO_2 sequestration by ureolytic microbial consortia through microbially-induced calcite precipitation, *Sci. Total Environ.*, 2016, **572**, 671–680.

19 M. Tepe, E. Arslan, T. Koralay and N. M. Doan, Precipitation and characterization of $CaCO_3$ of *Bacillus amyloliquefaciens* U17 strain producing urease and carbonic anhydrase, *Turk. J. Biol.*, 2019, **43**, 198–208.

20 B. D. Lee, W. A. Apel and M. R. Walton, Calcium carbonate formation by *Synechococcus* sp. strain PCC 8806 and *Synechococcus* sp. strain PCC 8807, *Bioresour. Technol.*, 2006, **97**, 2427–2434.

21 R. Ramanan, K. Kannan, A. Deshkar, R. Yadav and T. Chakrabarti, Enhanced algal CO_2 sequestration through calcite deposition by *Chlorella* sp. and *Spirulina platensis* in a mini-raceway pond, *Bioresour. Technol.*, 2010, **101**, 2616–2622.

22 W. Hou, B. Lian and X. Zhang, CO_2 mineralization induced by fungal nitrate assimilation, *Bioresour. Technol.*, 2011, **102**, 1562–1566.

23 S. Masaphy, L. Zabari, J. Pastrana and S. Dultz, Role of fungal mycelium in the formation of carbonate concretions in growing media—an investigation by SEM and synchrotron-based X-ray tomographic microscopy, *Geomicrobiol. J.*, 2009, **26**, 442–450.

24 A. C. Mitchell and F. G. Ferris, The influence of *Bacillus pasteurii* on the nucleation and growth of calcium carbonate, *Geomicrobiol. J.*, 2006, **23**, 213–226.

25 N. T. Enyedi, J. Makk, L. Kótai, B. Berényi, S. Klébert, Z. Sebestyén, Z. Molnár, A. K. Borsodi, S. Leél-Őssy, A. Demény and P. Németh, Cave bacteria-induced amorphous calcium carbonate formation, *Sci. Rep.*, 2020, **10**, 8696.

26 H. Li, Q. Yao, F. Wang, Y. Huang, S. Fu and G. Zhou, Insights into the formation mechanism of vaterite mediated by a deep-sea bacterium *Shewanella piezotolerans* WP3, *Geochim. Cosmochim. Acta*, 2019, **256**, 35–48.

27 Y. Y. Wang, Q. Z. Yao, H. Li, G. T. Zhou and Y. M. Sheng, Formation of vaterite mesocrystals in biomineral-like structures and implication for biomineralization, *Cryst. Growth Des.*, 2015, **15**, 1714–1725.

28 A. C. Mitchell, K. Dideriksen, L. H. Spangler, A. B. Cunningham and R. Gerlach, Microbially enhanced

carbon capture and storage by mineral-trapping and solubility-trapping, *Environ. Sci. Technol.*, 2010, **44**, 5270–5276.

29 C. Dupraz, R. P. Reid, O. Braissant, A. W. Decho, R. S. Norman and P. T. Visscher, Processes of carbonate precipitation in modern microbial mats, *Earth-Sci. Rev.*, 2009, **96**, 141–162.

30 A. J. Phillips, E. Lauchnor, J. Eldring, R. Esposito, A. C. Mitchell, R. Gerlach, A. B. Cunningham and L. H. Spangler, Potential CO_2 leakage reduction through biofilm-induced calcium carbonate precipitation, *Environ. Sci. Technol.*, 2013, **47**, 142–149.

31 R. Liu and B. Lian, Immobilisation of Cd(II) on biogenic and abiotic calcium carbonate, *J. Hazard. Mater.*, 2019, **378**, 120707.

32 Y. S. Kim, S. H. Kim, S. H. Cho and G. J. Lee, Effects of two formulation types of a microbial fertilizer containing *Bacillus Subtilis* on rowth of creeping bentgrass, *J. Int. Med. Res.*, 2014, **43**, 3–8.

33 F. O. T. S. Pérez Barrera and K. O. T. S. Akti, *Bacterial strain and composition used to accelerate composting and as a fertilizer*, EP1721966B1, 2009-10-28.

34 J. Han, B. Lian and H. Ling, Induction of calcium carbonate by *Bacillus cereus*, *Geomicrobiol. J.*, 2013, **30**, 682–689.

35 Y. Pocker and J. T. Stone, The catalytic versatility of erythrocyte carbonic anhydrase. III. kinetic studies of the enzyme-catalyzed hydrolysis of *p*-nitrophenyl acetate, *Biochemistry*, 1967, **6**, 668–678.

36 W. Li, P. Zhou, L. Jia, L. Yu, X. Li and M. Zhu, Limestone dissolution induced by fungal mycelia, acidic materials, and carbonic anhydrase from fungi, *Mycopathologia*, 2009, **167**, 37–46.

37 A. Moya, S. Tambutté, A. Bertucci, E. Tambutté, S. Lotto, D. Vullo, C. T. Supuran, D. Allemand and D. Zoccola, Carbonic anhydrase in the scleractinian coral *Stylophora pistillata* characterization, localization, and role in biomineralization, *J. Biol. Chem.*, 2008, **283**, 25475–25484.

38 X. Liu, W. Wang, M. Wang and P. Wang, Experimental study of CO_2 mineralization in Ca^{2+}-rich aqueous solutions using tributylamine as an enhancing medium, *Energy Fuels*, 2014, **28**, 2047–2053.

39 J. J. Lv, F. Ma, F. C. Li, C. H. Zhang and J. N. Chen, Vaterite induced by *Lysinibacillus* sp. GW-2 strain and its stability, *J. Struct. Biol.*, 2017, **200**, 97–105.

40 B. Sánchez, S. Chaignepain, J. Schmitter and M. C. Urdaci, A method for the identification of proteins secreted by lactic acid bacteria grown in complex media, *FEMS Microbiol. Lett.*, 2009, **295**, 226–229.

41 Y. Du, X. Zhou and B. Lian, The extracellular secretion of *Bacillus mucilaginosus* and its capability of releasing potassium from potassium-bearing minerals, *Earth Sci. Front.*, 2008, **15**, 107–111.

42 Z. Han, J. Wang, H. Zhao, M. E. Tucker, Y. Zhao, G. Wu, J. Zhou, J. Yin, H. Zhang, X. Zhang and H. Yan, Mechanism of biomineralization induced by *Bacillus subtilis* J2 and characteristics of the biominerals, *Minerals*, 2019, **9**, 218.

43 C. Rodriguez-Navarro, K. Kudłacz, Ö. Cizer and E. Ruiz-Agudo, Formation of amorphous calcium carbonate and its transformation into mesostructured calcite, *Crystengcomm*, 2015, **17**, 58–72.

44 A. Martignier, M. Pacton, M. Filella, J. M. Jaquet, F. Barja, K. Pollok, F. Langenhorst, S. Lavigne, P. Guagliardo and M. R. Kilburn, Intracellular amorphous carbonates uncover a new biomineralization process in eukaryotes, *Geobiology*, 2017, **15**, 240–253.

45 R. S. Rani and M. Saharay, Molecular dynamics simulation of protein-mediated biomineralization of amorphous calcium carbonate, *RSC Adv.*, 2019, **9**, 1653–1663.

46 A. Vecht and T. G. Ireland, The role of vaterite and aragonite in the formation of pseudo-biogenic carbonate structures: implications for Martian exobiology, *Geochim. Cosmochim. Acta*, 2000, **64**, 2719–2725.

47 R. S. K. Lam, J. M. Charnock, A. Lennie and F. C. Meldrum, Synthesis-dependant structural variations in amorphous calcium carbonate, *Crystengcomm*, 2007, **9**, 1226–1236.

48 F. Konrad, F. Gallien, D. E. Gerard and M. Dietzel, Transformation of amorphous calcium carbonate in air, *Cryst. Growth Des.*, 2016, **16**, 6310–6317.

49 Y. Cheng, F. Zhou, S. Li and Z. Chen, Removal of mixed contaminants crystal violet and heavy metal ions by immobilized stains as the functional biomaterial, *RSC Adv.*, 2016, **6**, 67858–67865.

50 C. Quintelas, Z. Rocha, B. Silva, B. Fonseca, H. Figueiredo and T. Tavares, Removal of Cd(II), Cr(VI), Fe(III) and Ni(II) from aqueous solutions by an *E. coli* biofilm supported on kaolin, *Chem. Eng. J.*, 2009, **149**, 319–324.

51 M. E. Argun and S. Dursun, A new approach to modification of natural adsorbent for heavy metal adsorption, *Bioresour. Technol.*, 2008, **99**, 2516–2527.

52 M. Ni and B. D. Ratner, Differentiation of calcium carbonate polymorphs by surface analysis techniques-an XPS and TOF-SIMS study, *Surf. Interface Anal.*, 2008, **40**, 1356–1361.

53 S. Yuan, M. Sun, G. Sheng, Y. Li, W. Li, R. Yao and H. Yu, Identification of key constituents and structure of the extracellular polymeric substances excreted by *Bacillus megaterium* TF10 for their flocculation capacity, *Environ. Sci. Technol.*, 2011, **45**, 1152–1157.

54 C. Yin, F. Meng and G. Chen, Spectroscopic characterization of extracellular polymeric substances from a mixed culture dominated by ammonia-oxidizing bacteria, *Water Res.*, 2015, **68**, 740–749.

55 X. Sun, S. Wang, X. Zhang, J. Paul Chen, X. Li, B. Gao and Y. Ma, Spectroscopic study of Zn^{2+} and Co^{2+} binding to extracellular polymeric substances (EPS) from aerobic granules, *J. Colloid Interface Sci.*, 2009, **335**, 11–17.

56 C. Zhang, F. Li and J. Lv, Morphology and formation mechanism in precipitation of calcite induced by *Curvibacter lanceolatus* strain HJ-1, *J. Cryst. Growth*, 2017, **478**, 96–101.

57 D. Ren, Q. Feng and X. Bourrat, Effects of additives and templates on calcium carbonate mineralization in vitro, *Micron*, 2011, **42**, 228–245.

58 G. Aloisi, A. Gloter, M. Krüger, K. Wallmann, F. Guyot and P. Zuddas, Nucleation of calcium carbonate on bacterial nanoglobules, *Geology*, 2006, **34**, 1017–1020.
59 S. Schultze-Lam, D. Fortin, B. S. Davis and T. J. Beveridge, Mineralization of bacterial surfaces, *Chem. Geol.*, 1996, **132**, 171–181.
60 Y. Politi, T. Arad, E. Klein, S. Weiner and L. Addadi, Sea urchin spine calcite forms *via* a transient amorphous calcium carbonate phase, *Science*, 2004, **306**, 1161–1164.
61 L. Gránásy, T. Pusztai, G. Tegze, J. A. Warren and J. F. Douglas, Growth and form of spherulites, *Phys. Rev. E: Stat., Nonlinear, Soft Matter Phys.*, 2005, **72**, 11605.
62 F. Li, H. Ma, N. Su, J. Wang, M. Liu, J. Wang and F. Teng, *Clostridium* sp. controlled morphology of Mg-bearing calcite and its implication for possible mechanism, *Geol. J. China Univ.*, 2011, **17**, 13–20.